

# Oxygen *K*-edge X-ray absorption spectra of liquids with minimization of window contamination

Linda I. Vogt,<sup>a</sup> Julien J. H. Cotelesage,<sup>a</sup> Charles J. Titus,<sup>b</sup> Samin Sharifi,<sup>c</sup> Albert E. Butterfield,<sup>c</sup> Peter Hillman,<sup>c</sup> Ingrid J. Pickering,<sup>a,d,\*</sup> Graham N. George<sup>a,d,\*</sup> and Simon J. George<sup>e,\*</sup>

Received 21 July 2021

Accepted 23 September 2021

Edited by R. W. Strange, University of Essex, United Kingdom

**Keywords:** oxygen *K*-edge X-ray absorption spectroscopy; spectroscopy of liquids; X-ray windows; oxygen contamination.

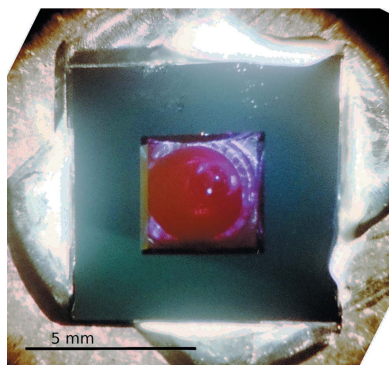
<sup>a</sup>Molecular and Environmental Sciences Group, Department of Geological Sciences, University of Saskatchewan, Saskatoon, Saskatchewan S7N 5E2, Canada, <sup>b</sup>Department of Physics, Stanford University, Stanford, CA 94305, USA, <sup>c</sup>Chevron Energy Technology Company, Richmond, CA 94802, USA, <sup>d</sup>Department of Chemistry, University of Saskatchewan, Saskatoon, Saskatchewan S7N 5C9, Canada, and <sup>e</sup>Simon Scientific, 2000 Allston Way, Unit 232, Berkeley, CA 94701, USA. \*Correspondence e-mail: ingrid.pickering@usask.ca, g.george@usask.ca, simon@simonscientific.com

Oxygen *K*-edge X-ray absorption spectroscopy is used routinely to study a range of solid materials. However, liquid samples are studied less frequently at the oxygen *K*-edge due to the combined challenges of high-vacuum conditions and oxygen contamination of window materials. A modular sample holder design with a twist-seal sample containment system that provides a simple method to encapsulate liquid samples under high-vacuum conditions is presented. This work shows that pure silicon nitride windows have lower oxygen contamination than both diamond- and silicon-rich nitride windows, that the levels of oxygen contamination are related to the age of the windows, and provides a protocol for minimizing the background oxygen contamination. Acid-washed 100 nm-thick silicon nitride windows were found to give good quality oxygen *K*-edge data on dilute liquid samples.

## 1. Introduction

Of all the chemical elements on Earth, oxygen is the most common by consideration of either mass or atomic abundance, with a crustal abundance of some 46.1 wt% (Lide, 2017). It is among the six major elements that are known to be essential for all life, and is involved in all manner of materials, ranging from high  $T_c$  superconductors to supported catalysts. Molecular oxygen, O<sub>2</sub>, comprising 20.95 wt% of our atmosphere (Lide, 2017), is highly reactive and second only to fluorine in terms of electronegativity (e.g. Pauling, 1960). As a direct consequence of this, many materials have passivation layers comprising oxides, which can create challenges in the spectroscopic study of oxygen chemistry (Fрати *et al.*, 2020).

O *K*-edge X-ray absorption spectroscopy (XAS) has been widely used as a sensitive probe of chemical speciation and electronic structure in a range of materials (Fрати *et al.*, 2020). In common with other soft X-ray measurements, and as a consequence of the low penetration of the beams at these energies, experiments at the O *K*-edge often need to be conducted under high vacuum. An added complication is that oxygen measurements are frequently distinguished compared with measurements of other edges at similar energies by contamination issues due to both the prevalence and the reactivity of oxygen. In some cases oxygen contamination issues have led to apparently conflicting experimental results. For example, early work using O *K*-edge XAS formulated lithium nickel oxides, Li<sub>x</sub>Ni<sub>(1-x)</sub>O, as formal Ni(II) species with hole states localized at oxygen (van Elp *et al.*, 1992), whereas



Ni *K*-edge XAS studies suggested that the reverse was true, with hole states on the nickel and a formal Ni(III) oxidation state (Pickering *et al.*, 1993). More recent work has shown that these materials are better understood as Ni(III) complexes (Green *et al.*, 2020) and that early challenges with oxygen XAS arose from surface contamination.

To date, sample conditions have ranged from cryogenic to the solid state (Frati *et al.*, 2020), but relatively few static liquid and solution samples have been investigated (Vogt *et al.*, 2020) due to the combined challenges of handling liquids under high-vacuum conditions and oxygen contamination of window materials (Frati *et al.*, 2020). Herein we present a design for a high-vacuum-compatible liquid solution sample system employing silicon nitride windows, together with a study of the oxygen contamination issues of the system.

## 2. Materials and methods

### 2.1. X-ray absorption spectroscopy

O *K*-edge XAS measurements were carried out using the Stanford Synchrotron Radiation Lightsource (SSRL, Menlo Park, CA, USA) on beamline 10-1 with the spherical grating monochromator employing the 600 lines mm<sup>-1</sup> grating. Fluorescence yield spectra were measured using a 240 pixel transition edge sensor (TES) array detector (Lee *et al.*, 2019) with the intensity of the incident beam measured as the drain current from an electrically isolated evaporated gold mesh upstream of the sample. Conductive carbon adhesive tape

(Agar Scientific, Stanstead, Essex, UK) and indium metal strips (Goodfellow Metals, Cambridge, UK) were mounted directly onto the sample holder. Indium was cleaned by washing in acetone and isopropyl alcohol followed by etching with 10 wt% hydrochloric acid (Sigma–Aldrich Chemical Company, St Louis, MI, USA) for 1 min. Calibration of the incident X-ray energy was with reference to a Ti<sub>2</sub>O<sub>3</sub> standard and assumed an energy of 531.0 eV for the maximum of the lowest-energy O *K*-edge XAS peak.

### 2.2. Sample holder design

The sample holder design employed a rod of standard dimensions for SSRL beamline 10-1, but with four removable side panels held in place with bolts (Fig. 1). The side panels were milled to accommodate samples via a front-loading 1.5 mm diameter, 5 mm deep central well with an indented surface which fitted a window. The side panels could optionally be gold-plated to reduce surface oxygen contamination from the passivation layer. The top and bottom of the central aluminium rod were drilled and threaded allowing for the attachment of a magnetic mount (top) and a spill tray (bottom). All metal parts of the sample holder system were thoroughly cleaned and de-greased with solvent (dichloromethane) before use. All tapped parts were vented to reduce purge times while in use in the high-vacuum environment.

Each sample was encapsulated using an X-ray transparent thin window using vacuum-compatible epoxy cement (Thorlabs Inc. Newton, NJ, USA). Initially, epoxy cement was laid



**Figure 1** Modular sample holder. The left diagram shows an exploded view of the modular sample holder showing locations for sample in each of the four different side panels. The top right shows the twist-seal sample holder design, from left to right, without a window, without window plus epoxy (white), with a window in the initial load position and with a window in the twist-sealed position. The lower right panel shows a photograph of a sample (pink) contained within a sample holder encapsulated by a window.

out in an incomplete ring or ‘horseshoe’ in the indent around the sample well (Fig. 1). Following this, the liquid sample was placed in the central well using a pipette or syringe. The window, held by soft-tipped forceps, was placed with one edge inclined at a slight angle above the gap in the epoxy cement. The window was pressed gently into the epoxy and then was rotated to spread the epoxy, thus sealing the sample cell (Fig. 1). The epoxy was cured for a minimum of 24 h under an atmosphere of argon before the panels were mounted on the central aluminium rod. The twist-seal sample holder design allows a minimum of epoxy cement to be used, which helps reduce out-gassing, and allows the required vacuum to be achieved ( $\sim 10^{-8}$  Torr for SSRL BL 10-1). The design also allows for fragile 100 nm-thick windows to be easily used and mounted without breakage.

### 2.3. X-ray windows

Three different commercial window materials were examined in the course of this work – diamond (Applied Diamond Inc. Wilmington, DE, USA), silicon nitride ( $\text{Si}_3\text{N}_4$ ) (Silson Ltd, Southam, Warwickshire, UK) and silicon-rich nitride (often abbreviated to  $\text{SiN}_x$ ) (Norcada Inc. Edmonton, Alberta, Canada).

### 2.4. Acid washing of windows

A commercial hydrofluoric acid etching solution was used [Buffered oxide etchant (BOE) 10:1, Sigma–Aldrich Chemical Company, St Louis MI, USA] diluted with deionized water to produce a 1 wt% hydrofluoric acid solution. Windows were exposed to the etching solution for varying times, and then rinsed in three consecutive deionized water baths for 20 s each in order to remove any adherent hydrofluoric acid. Treated windows were allowed to dry under an atmosphere of argon.

**WARNING:** Hydrofluoric acid poses serious safety risks and should only be used in a fume hood by experimenters wearing personnel protective equipment. Hydrofluoric acid is both highly corrosive and a contact poison. Exposure can cause serious burns to the skin or other tissues, with serious complications due to toxicity.

## 3. Results and discussion

The modular twist-seal sample holder design allows a series of samples to be mounted in the beamline and examined sequentially.

With liquid samples the high-vacuum conditions of SSRL beamline 10-1 requires the use of X-ray transparent windows, and the low X-ray energies of the O *K*-edge requires necessarily thin windows. In order to ascertain the oxygen contamination levels of the windows, tests of the windows were conducted without using the sample holder described in Section 2.2, in a sample geometry that permitted illumination of the window alone with no potentially contaminated metal surfaces behind.

All windows were 100 nm thick, and were provided mounted on a supporting frame by the vendors. X-ray trans-

mission of the windows at the O *K*-edge energy is approximately 0.680 (0.667) and 0.679 (0.667) for pure  $\text{Si}_3\text{N}_4$  and diamond, respectively, with the values in parentheses being the transmission at the O *K* $\alpha$  energy. The use of thicker and hence mechanically more robust windows, such as commercially available 200 nm windows, would reduce the X-ray transmission below 50%, reducing the signal too much and hence is precluded for our applications.

Silicon-rich nitride is widely used in the opto-electronics industry (*e.g.* Papet *et al.*, 2006; Tao *et al.*, 2015) and initially was preferred for our application due to its better mechanical properties compared with pure  $\text{Si}_3\text{N}_4$  (lower inherent stress and less brittle). Fig. 2 compares the O *K*-edge XAS spectra of three types of windows, together with spectra obtained from metallic indium and carbon adhesive tape, both of which are used routinely in measurements of concentrated solids. All three window types show substantial oxygen contamination, with higher levels for diamond and silicon-rich nitride. Because of this, the majority of our investigations focused on  $\text{Si}_3\text{N}_4$  windows.

It is common practice for vendors to stockpile windows and store them, often for years, with only minimal precautions against air exposure. Thus, purchase of windows can involve uncertainty in the age of the product that will be received, and we therefore investigated whether the time since manufacture might be related to oxygen contamination. Windows of a range of manufacture dates were requested from manufacturers, with XAS measured from windows spanning more than two decades of age. A clear correlation of oxygen levels with the time since window manufacture (Fig. 2, inset) demonstrates that oxygen contamination accumulates with time, initially rapidly, and then slowly. In freshly manufactured windows for which the vendor had employed anaerobic conditions for shipping and storage, the contamination was smaller but still present. We therefore examined the use of acid washing of the windows in order to help reduce the oxygen contamination prior to use in our sample cell. Of the readily available acids, hydrofluoric acid is a standard in the semiconductor industry as the only wet-chemical medium that can etch silicon dioxide at a reasonable rate; hydrochloric acid does not react with silicon dioxide, while oxo-acids compound oxygen contamination. We also considered the alternative approach of using argon-milling to remove the outer oxide layer, but rejected this as it is likely to significantly stress and weaken the thin  $\text{Si}_3\text{N}_4$  windows.

Tests were carried out to determine whether hydrofluoric acid etching solution could remove oxygen contamination; initial tests using 0.1 wt% hydrofluoric acid were ineffective, and windows were treated with 1 wt% hydrofluoric acid etching solution. Fig. 3 shows vertical sample positioner scans of a series of windows dipped in hydrofluoric acid for different times, with the TES detector monitoring nitrogen, oxygen and fluorine *K* $\alpha$  X-ray fluorescence employing an incident X-ray energy of 530 eV, at the expected O *K*-edge maximum, to excite oxygen and below. The incident X-ray beam contained sufficient second harmonic to excite fluorine. The oxygen window contamination decreased with acid exposure time,

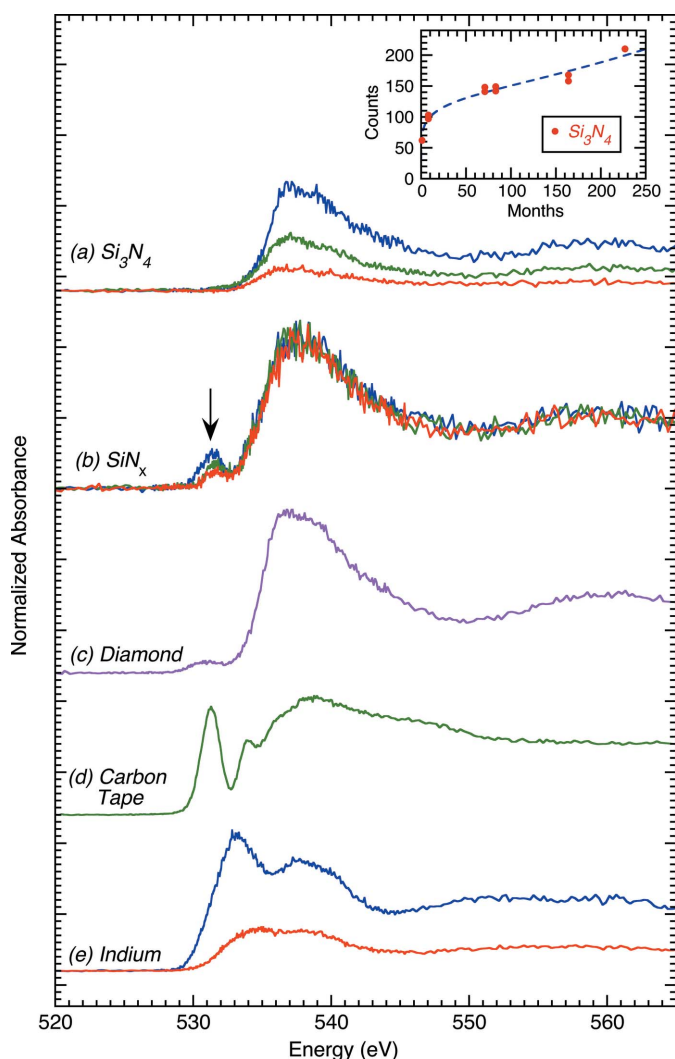


**Figure 2**  
 O  $K$ -edge spectra of 100 nm-thick windows and other materials used for O  $K$ -edge measurements. All spectra were measured using partial fluorescence yield and have been normalized except as noted. (a) Stoichiometric silicon nitride windows: blue – after storage for some months, green – freshly manufactured, stored under argon and measured within 2 weeks, red – after 10 s hydrofluoric acid washing. These spectra are normalized to the same scale as the silicon-rich nitride spectra in (b). (b) Silicon-rich nitride windows showing the time-dependence of the pre-edge structure (arrowed): blue – first scan, green and red – subsequent scans. (c) Diamond windows. We note that the intensity of this signal is about double that of silicon-rich nitride. (d) Carbon tape. (e) Pressed indium: blue – as supplied, red – after cleaning via washing in solvents and an acid etch. These spectra are normalized to the same scale.

with the nitrogen fluorescence acting as an indicator of window thickness. The optimum acid exposure time, maximizing oxygen contamination removal without compromising the window, was determined to be 20 s.

Our study of different window materials clearly indicated that considering both oxygen contamination and mechanical rigidity perspectives the best overall material was  $\text{Si}_3\text{N}_4$  with a 20 s 1% hydrofluoric acid wash. The oxygen contamination of the silicon-rich nitride ( $\text{SiN}_x$ ) windows proved sensitive to radiation exposure [Fig. 2(b)], with a low-energy  $\pi^*$  feature reducing and changing with prolonged exposure, which lies a

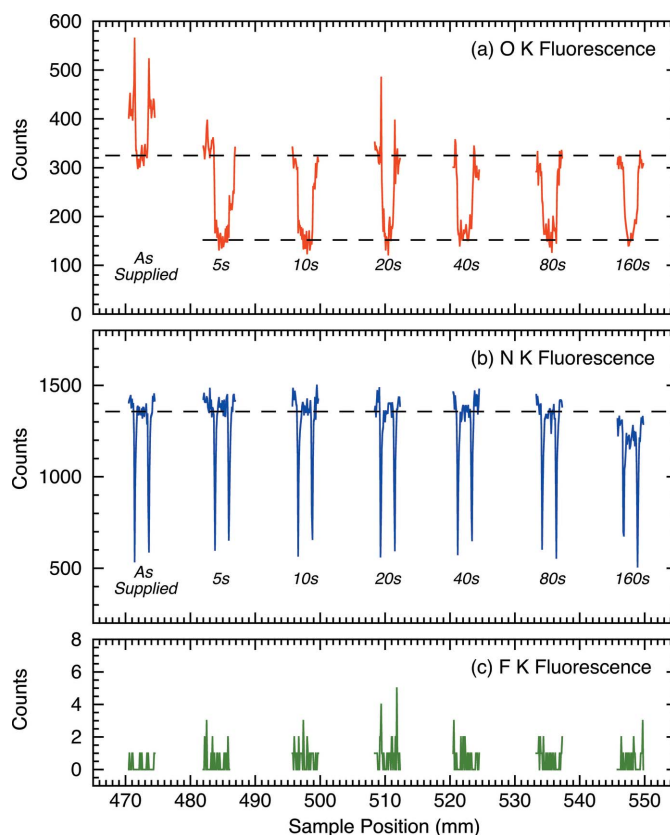


**Figure 3**  
 Effectiveness of hydrofluoric acid washing of stoichiometric silicon nitride windows. Vertical scan of a series of freshly made windows with different hydrofluoric acid wash times showing changes in (a) O, (b) N and (c) F content via X-ray fluorescence. We note that both sides of the silicon frame are covered with silicon nitride, with silicon exposed only around the window on the etched side. This is apparent in the N  $K$ -edge profile, where the window area is bounded by two sharp reductions in N  $K$ -fluorescence. A 5 s or longer hydrofluoric acid wash reduces the O  $K$ -edge fluorescence by over  $\sim 50\%$ , presumably removing the surface oxide layer and leaving bulk adsorbed O. Etching of the silicon nitride window is observed after 80 s through loss of the N  $K$ -fluorescence. Minimal residual F is seen, showing the water washing steps are sufficient.

little below the energy of the  $1s \rightarrow \pi^*$  transition of carbonyl ( $\text{C}=\text{O}$ ). Preliminary calculations indicate that the analogous transition energy for an  $\text{Si}=\text{O}$  group would be expected to fall at approximately 0.6 eV lower energy than for  $\text{C}=\text{O}$ . Irrespective of its origins the X-ray dose-dependent background spectrum is an additional factor which argues against the use of  $\text{SiN}_x$  windows.

The use of acid-washed  $\text{Si}_3\text{N}_4$  windows reduces the oxygen contamination signal, but does not completely eliminate it, requiring the use of difference spectra for the most dilute samples. The spectrum of a dilute hydrocarbon-based sample containing trace amounts of oxygen is shown in Fig. 4, together with the blank spectrum taken using an acid-washed  $\text{Si}_3\text{N}_4$  window sample in isolation.

Our twist-seal sample holder design provides a simple method for encapsulating liquid samples under high-vacuum conditions which are frequently required for soft X-ray spectroscopy experiments. Although designed for the O  $K$ -edge, it would work equally well for measuring spectra on liquids with

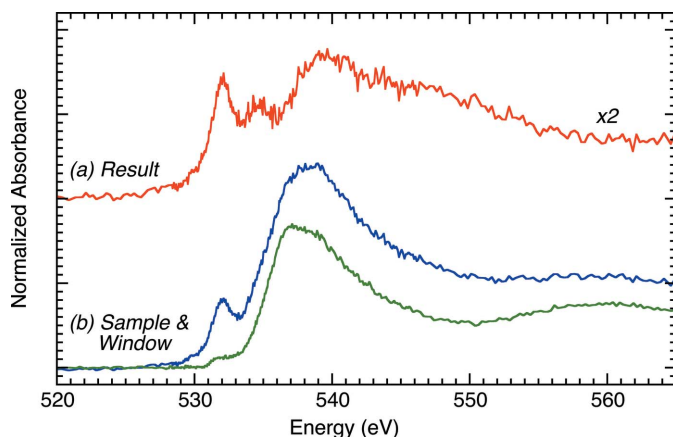


**Figure 4**

O *K*-edge XAS of a dilute complex oxygen-containing liquid using our sample cell with a 100 nm-thick Si<sub>3</sub>N<sub>4</sub> window. The window and the sample were measured separately and subtracted. (a) Difference spectrum representing the pure spectrum of the sample. (b) Blue – sample measurement, green – baseline (window) measurement. All spectra are normalized to the same scale – with the difference spectrum vertically scaled by a factor of two for clarity.

other absorption edges in this energy regime. We have also provided a protocol for minimizing the background oxygen contamination, allowing studies of the O *K*-edge of dilute samples. While our initial application was targeted towards investigation of static samples, our design could be readily modified to accommodate either a flow system or an electrochemical system for *operando*-type studies.

### Funding information

The following funding is acknowledged: Chevron Energy Technology Company (contract to GNG, IJP and SJG); Natural Sciences and Engineering Research Council of Canada (grant No. RGPIN-2016-05810 awarded to IJP; grant

No. RGPIN-2019-05351 awarded to GNG); Canada Research Chairs (awarded to IJP and GNG). Use of the Stanford Synchrotron Radiation Lightsource (SSRL), SLAC National Accelerator Laboratory, is supported by the US Department of Energy (DOE), Office of Science, Office of Basic Energy Sciences (contract No. DE-AC02-76SF00515).

### References

- Elp, J. van, Eskes, H., Kuiper, P. & Sawatzky, G. A. (1992). *Phys. Rev. B*, **45**, 1612–1622.
- Fрати, F., Hunault, M. O. J. Y. & de Groot, F. M. F. (2020). *Chem. Rev.* **120**, 4056–4110.
- Green, R. J., Wadati, H., Regier, T. Z., Achkar, A. J., McMahon, C., Clancy, J. P., Dabkowska, H. A., Gaulin, B. D., Sawatzky, G. A. & Hawthorn, D. G. (2020). arXiv:2011.06441v1.
- Lee, S.-J., Titus, C. J., Alonso Mori, R., Baker, M. L., Bennett, D. A., Cho, H. S., Doriese, W. B., Fowler, J. W., Gaffney, K. J., Gallo, A., Gard, J. D., Hilton, G. C., Jang, H., Joe, Y. I., Kenney, C. J., Knight, J., Kroll, T., Lee, J.-S., Li, D., Lu, D., Marks, R., Minitti, M. P., Morgan, K. M., Ogasawara, H., O’Neil, G. C., Reintsema, C. D., Schmidt, D. R., Sokaras, D., Ullom, J. N., Weng, T.-C., Williams, C., Young, B. A., Swetz, D. S., Irwin, K. D. & Nordlund, D. (2019). *Rev. Sci. Instrum.* **90**, 113101.
- Lide, D. R. (2017). *CRC Handbook of Chemistry and Physics*, edited by W. M. Haynes, 97th ed., pp. 14–17. Boca Raton: CRC Press.
- Papet, P., Nichiporuk, O., Kaminski, A., Rozier, Y., Kraiem, J., Lelievre, J.-F., Chaumartin, A., Fave, A. & Lemiti, M. (2006). *Sol. Energy Mater. Sol. Cells*, **90**, 2319–2328.
- Pauling, L. (1960). *The Nature of the Chemical Bond*, 3rd ed. Ithaca: Cornell University Press.
- Pickering, I. J., George, G. N., Lewandowski, J. T. & Jacobson, A. J. (1993). *J. Am. Chem. Soc.* **115**, 4137–4144.
- Tao, S. X., Theulings, A. M. M. G., Prodanović, V., Smedley, J. & van der Graf, H. (2015). *Computation*, **3**, 657–669.
- Vogt, L. I., Cotelesage, J. J. H., Dolgova, N. V., Titus, C. J., Sharifi, S., George, S. J., Pickering, I. J. & George, G. N. (2020). *RSC Adv.* **10**, 26229–26238.